Amphiphilic Block Copolymers Based on PEG and UV-Triggerable Self-Immolative Polymers

Adám Viktor Joó, Jonathan Potier, Nouzha Ouhssou, Bárbara Pepino Mendes, Gaëlle Le Fer, Patrice Woisel, Kedafi Belkhir

Amphiphilic Block Copolymers based on PEG and UV-Triggerable Self-Immolative Polymer

Ádám Viktor Joó, Jonathan Potier, Nouzha Ouhssou, Bárbara Pepino Mendes, Gaëlle Le Fer, Patrice Woisel, Kedafi Belkhir*

Univ. Lille, CNRS, INRAE, Centrale Lille, UMR 8207-UMET-Unité Matériaux et Transformations, F-59000 Lille, France

Corresponding author: Kedafi Belkhir, kedafi.belkhir@centralelille.fr

ABSTRACT

Self-Immolative polymers (SIPs) allow a triggered depolymerization which is an effective way to control the function of polymer-based systems. In this work, hydrophobic SIP segments and hydrophilic polyethylene glycol (PEG) are combined in diblock and triblock amphiphilic architectures, the SIP-based blocks are made of polycaprolactone-like backbones with UV-sensitive nitrobenzene pendent groups. The depolymerization of the designed architectures in solution is monitored by NMR, UV-vis spectroscopy and size exclusion chromatography, showing complete cleavage of the triggering units in the SIP parts after about 25 minutes under UV-irradiation, and depolymerization rates of the SIP backbones up to 60%. Self-assemblies are prepared from the diblock copolymers, their stability is verified by DLS, and the UV-triggered disintegration of the self-assemblies is demonstrated by SEM, Tindall Effect and by monitoring the derived count rate in DLS, showing a rapid disintegration (after 2 to 6 minutes under UV light). These SIP-based structures allow a fast, controlled and on-demand disintegration of self-assemblies, with the ability to encapsulate and release on-demand the Nile red as hydrophobic model molecule.

KEYWORDS: Triggered Depolymerization, Self-Immolative Polymers, UV-Responsive Polymers, Self-Assemblies.

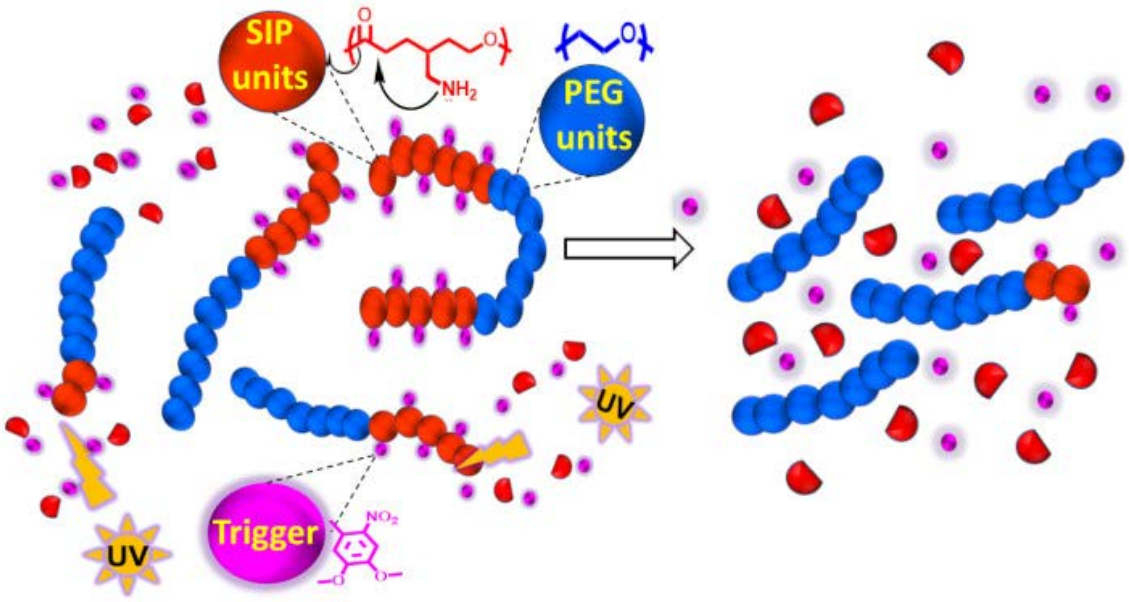

INTRODUCTION

Temporary polymer-based structures demonstrated their effectiveness in many advanced fields of polymer science, especially in technologies related to health and biomedical applications.[1-3] In these fields, the main feature of polymer-engineered temporary structures is the ability to be shaped in a desired manner and scale, especially in the form of nanoparticles, and then to be degraded. This degradation can be achieved either through a polymer chain biodegradation reaction or in response to an external stimulus[4,5]. This has enabled the development of a variety of drug vectors.[6–8]

Biodegradable polymers, i.e. polymers that can be completely degraded in natural environment by the action of microorganisms, such as poly(lactic acid) and polycaprolactone, are extensively investigated to develop these structures[9,10] but nevertheless with some drawbacks. The most limiting factor is the difficulty of controlling their degradation kinetics, which are highly dependent on the surrounding conditions[11], such as pH,[12] moisture content, and temperature.[13] Although it is possible

to prolong or accelerate the degradation process by choosing polymers with slow or fast biodegradation kinetics, respectively, this method remains empirical and once implemented, it is no longer possible to control the degradability of such systems.

To overcome this issue, stimuli-responsive polymers were widely explored to develop temporary self-assemblies that can be degraded using external stimulus on demand.[14–16] In this context, polymers with different chemical structures and sensitivities to various external stimuli have been proposed. Among these stimuli, UV light has shown many advantages, such as remote action, localized application, adjustable intensity, and on/off switching.[17,18]

Many efforts have been made to prepare UV-sensitive polymer-based self-assemblies with different mechanisms of degradation, including decrosslinking of the core of the self-assemblies,[19,20] isomerization,[21] cleavage of chromophores etc. all these mechanisms lead to the disruption of the assemblies. Recently, a class of polymers, called self-immolative polymers (SIPs),[22–24] have been distinguished by their ability to translate an external stimulus into a controlled depolymerization reaction of their backbone, thus providing predictable disassembly profiles. However, few studies were dedicated to incorporate SIPs within macromolecular architectures such as amphiphilic block copolymers. Recently Gillies and co-workers[25] synthesized stimuli-responsive amphiphilic copolymers, the diblock architectures were triggerable by both UV-light and acidic medium. The sensitivity to low pH was provided by the hydrophilic block of poly(ethylglyoxylate), while the hydrophobic block contains a single UV-sensitive triggering unit at the chain end (nitrobenzene). When the structures were exposed to the stimuli, the depolymerization occurs following a head-to-tail successive cleavage (cascade depolymerization). These copolymers allowed the preparation of self-assemblies that can be dissociated in response to either UV light or acidity. The kinetics of the depolymerization and

disassembling were of order of a few days. Liu and co-workers[26] prepared diblock amphiphilic architectures in which the hydrophilic block was PEG and the hydrophobic one was a SIP, bearing a single triggerable unit at the chain-end. The stimuli were reactive oxygen species and acidic medium, the depolymerization kinetics were of the order of a day (24 hours). The current work aims to develop UV-responsive SIP-based self-assemblies with faster dissociation kinetics and higher level of control. To reach this purpose, a different strategy is followed and consists of incorporating hydrophobic SIP segments with multiple triggering units, rather than unique one as in the cited works, thus the cleavage events in the different units of the SIP chains are supposed to take place independently from each other.

Amphiphilic di- and triblock copolymers will be developed in this work, using PEG as hydrophilic block and a SIP as hydrophobic one. The structure of SIP blocks used here contains a UV-sensitive pendent trigger on each repeating unit of the backbone, they belong to the category of chain-shattering self-immolative polymers[27,28]. These SIPs translate the external stimulus into multiple cleavage events that occurs, independently of each other, at different parts of the backbone, leading to faster kinetics and higher level of depolymerization control. The macromolecular architectures are designed to be amphiphilic in order to make self-assemblies in solution, with the possibility to break them by UV light. A facile synthesis method is proposed here to obtain the copolymers, leading to a simple method for the preparation of the UV-responsive nanoparticles.

MATERIALS AND METHODS

Materials

4-N-boc-aminomethylcyclohexanone (Boc-NH, 95%) was purchased from Enamine, Latvia. N,N-diisopropylethylamine (DIEA, 99%), dimethyl sulfide (DMS, 99+%), 4-

nitrophenyl chloroformate (pNPCL, 97%), 3-chloroperoxybenzoïc acid (*m*CPBA, 70-75%) and diphenyl phosphate (DPP, 99%) were purchased from Thermo Fisher Scientific, France. 4,5-Dimethoxy-2-nitrobenzyl alcohol (DMNBA, 98%) and dimethylformamide (DMF, 99.99%) were purchased from Carlo Erba, France. Polyethylene glycol methyl ether (CH_3-PEG-OH, 2000 $g.mol^{-1}$) and polyethylene glycol (HO-PEG-OH, 4000 $g.mol^{-1}$) were purchased from TCI, Belgium. Dry toluene was obtained by distillation over sodium. Deuterated chloroform was purchased from Eurisotop France.

Syntheses procedures

Monomer synthesis: The monomer (compound **4**) was synthesized according to a three-step synthesis procedure, all of them are detailed in Supporting Information S1.

Synthesis of amphiphilic diblock and triblock copolymers: the diblock and triblock copolymers were synthesized by ring opening polymerization (ROP) of **4** using CH_3-PEG-OH and HO-PEG-OH as initiators, respectively. Cylindrical glassware pressure vessel (tube) was dried in an oven at 70°C overnight and then cooled under nitrogen flow. The initiator (PEG) and the monomer powder were dried under vacuum for 24 hours and then introduced in the tube. Dry toluene was then added and the mixture was stirred for 1 hour before DPP was added as catalyst. The tube was sealed and the mixture was heated to 155°C in an oil bath. After 6 hours the reaction medium was diluted by adding chloroform, then the solvents were removed under reduced pressure, the resulting crude brown product was analyzed by ^{1}H NMR to determine the monomer conversion. The crude product was then solubilized in dichloromethane and precipitated first in hexane before being solubilized again in dichloromethane and precipitated in diethyl ether. A brownish product was obtained and dried under vacuum

for 12 hours. The amounts of the reagents used for the synthesis of each copolymer, with the expected structures, are detailed in Table 1.

Table 1. Amounts of the different reagents used to synthesize the copolymers.

	Expected structure*	CH_3-PEG-OH	HO-PEG-OH	Monomer**	DPP
Diblocks	PEG_{2000}-b-SIP_{2000}	0.436 g, 1 eq	/	0.5 g, 6 eq	0.054 g, 1 eq
	PEG_{2000}-b-SIP_{4000}	0.218 g, 1 eq	/	0.5 g, 12 eq	0.027 g, 1 eq
Triblocks	SIP_{2000}-b-PEG_{4000}-b-SIP_{2000}	/	0.436 g, 1 eq	0.5 g, 12 eq	0.054 g, 2 eq
	SIP_{4000}-b-PEG_{4000}-b-SIP_{4000}	/	0.218 g, 1 eq	0.5 g, 24 eq	0.027 g, 2 eq

*The subscript values refer to the expected molar masses of the different segments.

**The monomer concentration was 0.5 $g.mL^{-1}$ for all the runs (1 mL toluene was used as solvent).

^{1}H NMR analyses

^{1}H NMR spectra were recorded using a 300 MHz Bruker spectrometer. Deuterated chloroform ($CDCl_3$) was used as solvent and tetramethylsilane as reference at 0 ppm.

Size Exclusion Chromatography (SEC)

SEC measurements were carried out in a Waters chromatography system equipped with three columns connected in series (Styragel HR1, Styragel HT4 and Styragel HT4) and a refractive index detector (RI). The eluant was dimethylformamide (DMF) containing toluene (1 wt.%) and LiBr salt (1 $g.L^{-1}$). The copolymer samples were first stirred in the eluent solution until complete dissolution (~ 7 $mg.mL^{-1}$), then filtrated through a 0.45 µm pore-size PTFE filters before injection in the columns.

Preparation of self-assemblies

Two methods were followed to prepare the self-assemblies:

The direct nanoprecipitation method:[29] the copolymer was first solubilized in dichloromethane (1 $mg.mL^{-1}$, magnetic stirring for 24 hours), then 2 mL of the solution were slowly added to 2 mL of ethanol by using a syringe pump at a rate of 0.5 $mL.h^{-1}$, while being magnetically stirred. The obtained mixture was stirred for 2 hours, then the dichloromethane was removed in rotavapor. The resulting copolymer/ethanol suspension (1 $mg.mL^{-1}$) was stirred for 24 hours before characterizations.

The direct dissolution: the copolymer was directly mixed with distilled water (1 $mg.mL^{-1}$) and magnetically stirred for 24 hours at room temperature before characterization. This method is used here to show the ability of the copolymers to self-assemble by a one-step facile method, without using organic solvents. According to literature[30], only a limited number of copolymers can undergo self-assembling by simple dissolution in water.

UV irradiation

The irradiation of the samples was carried out in the UV chamber of the LZC-4V photoreactor from Luzchem Research Inc. Canada. 14 UV lamps are arranged on the internal walls of the chamber, the maximum emission wavelength of the lamps was 352 nm, the total power of irradiation was 1.3 $mW.cm^{-2}$ (measured by a power meter). For the monitoring of the depolymerization, each sample was dissolved in chloroform (1 $mg.mL^{-1}$) and stirred under UV irradiation during the appropriate time. The disassembling kinetics under UV irradiation was investigated on suspensions (in water or ethanol) of self-assemblies under stirring.

Dynamic Light Scattering (DLS)

The diameter of the self-assemblies and the derived count rate were measured by DLS, using a Zetasizer Ultra from Malvern, France. The temperature was set to 25°C for all the measurements.

Scanning Electron Microscopy (SEM)

SEM images were recorded using a Hitachi SU 5000 microscope, in EDS mode, with 10-30 kV accelerating voltage. Metallic spots were polished, then a drop of sample (suspension of self-assemblies) was spread on the spot. After evaporating the solvent, the sample was subjected to metallization treatment using the Precision Etching and Coating System (PECS) 682 Gatan, USA, allowing the deposition of regular and thin layer of chrome on the sample.

UV-vis absorption measurements

UV-vis absorption measurements were carried out on a Cary 3500 spectrophotometer from Agilent. The sample was placed in a 10 mm width cuvette, and the scan is achieved between 300 and 600 nm.

Fluorescence measurements

Fluorescence emission intensity measurements were performed using a Cary Eclipse Fluorescence spectrometer from Agilent. The excitation wavelength was 555 nm.

RESULTS AND DISCUSSION

Synthesis of the monomer and the copolymers

The ^{1}H NMR spectra corresponding to the monomer, and the different steps of its synthesis, are in Supporting Information Scheme S1 and Figures S1 to S4.

The synthetic schemes of the ROPs are summarized in scheme 1.

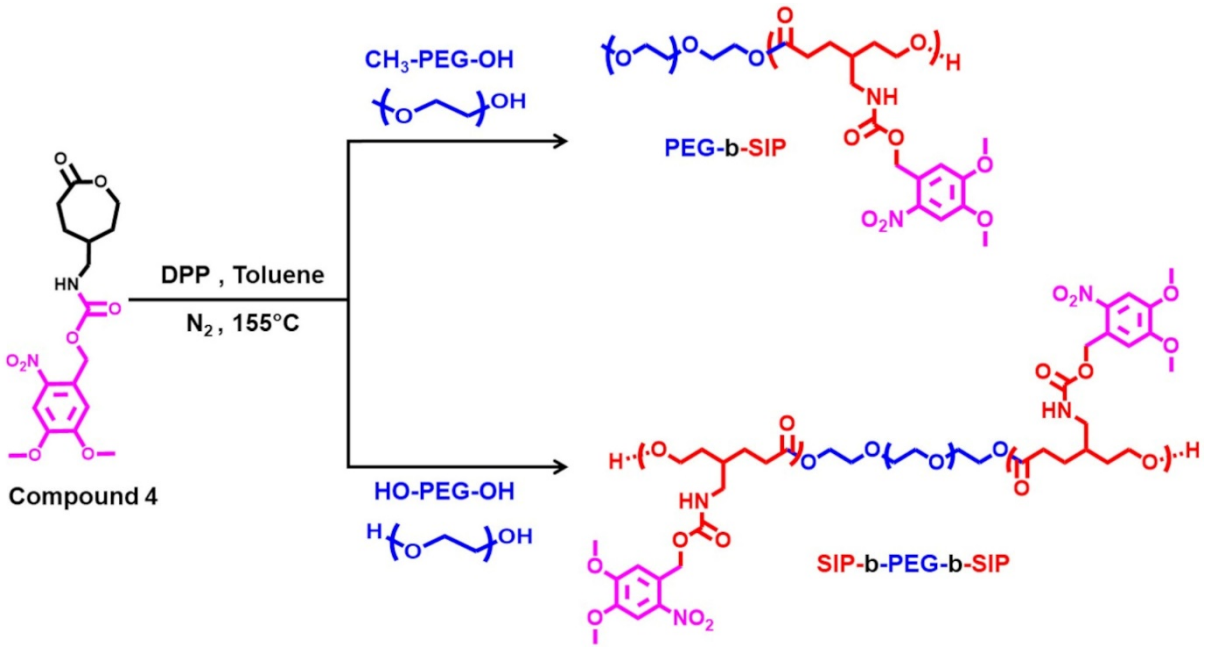

Scheme 1. Schemes of the synthesis of the diblock and triblock copolymers by ROP of Compound 4.

Monomer conversion was calculated for all the polymerizations by ^{1}H NMR (for details on calculation see Supporting Information, Figure S5). The results are summarized in Table 2 and show high conversions, going up to 89%.

After purification, the four copolymers were analyzed by ^{1}H NMR. The spectra of PEG_{2000}-b-SIP_{4000} and SIP_{4000}-b-PEG_{4000}-b-SIP_{4000} as representative diblock and triblock models, respectively, are shown in Figure 1. The methyl group at the chain-end of the PEG segment in the diblock structure is reflected by the peak ‘a’ at 3.40 ppm, as expected this peak does not appear in the spectrum of the triblock structure. The protons of the PEG backbone show two signals in both di- and triblock structures, the first at 3.66 ppm corresponds to b and c protons, and the second at 4.15 ppm includes the protons d and e. For the SIP segments, signals appear corresponding to the protons of the backbone formed after the ROP (protons g,h,i,j,k and f), the protons l,m,n and o correspond to the triggering units and appears respectively at 5.44, 3.99,

6.99 and 7.63 ppm. To check if the expected lengths of the SIP segments have been reached, the degree of polymerization (DP) was calculated from these spectra by integrating the peaks of the polymerized SIP units and comparing them to the peak of PEG (peak of the protons b and c in Figure 1). The peak k at 3.17 ppm was chosen for the SIP unit, with consideration of the next steps of this study (this peak does not interfere with the peaks of the products resulting from the UV-depolymerization of the SIP parts). The calculated DP values are summarized in Table 2 for both diblocks and triblocks. SEC analyses were also performed on the copolymers (the traces are in Supporting Information Figure S6) and showed, as expected, shorter elution times for the copolymers than for the macroinitiators (CH_3-PEG-OH and HO-PEG-OH) confirming the increase in molecular weight. Low dispersity values were obtained (<1.3) as shown in Table 2.

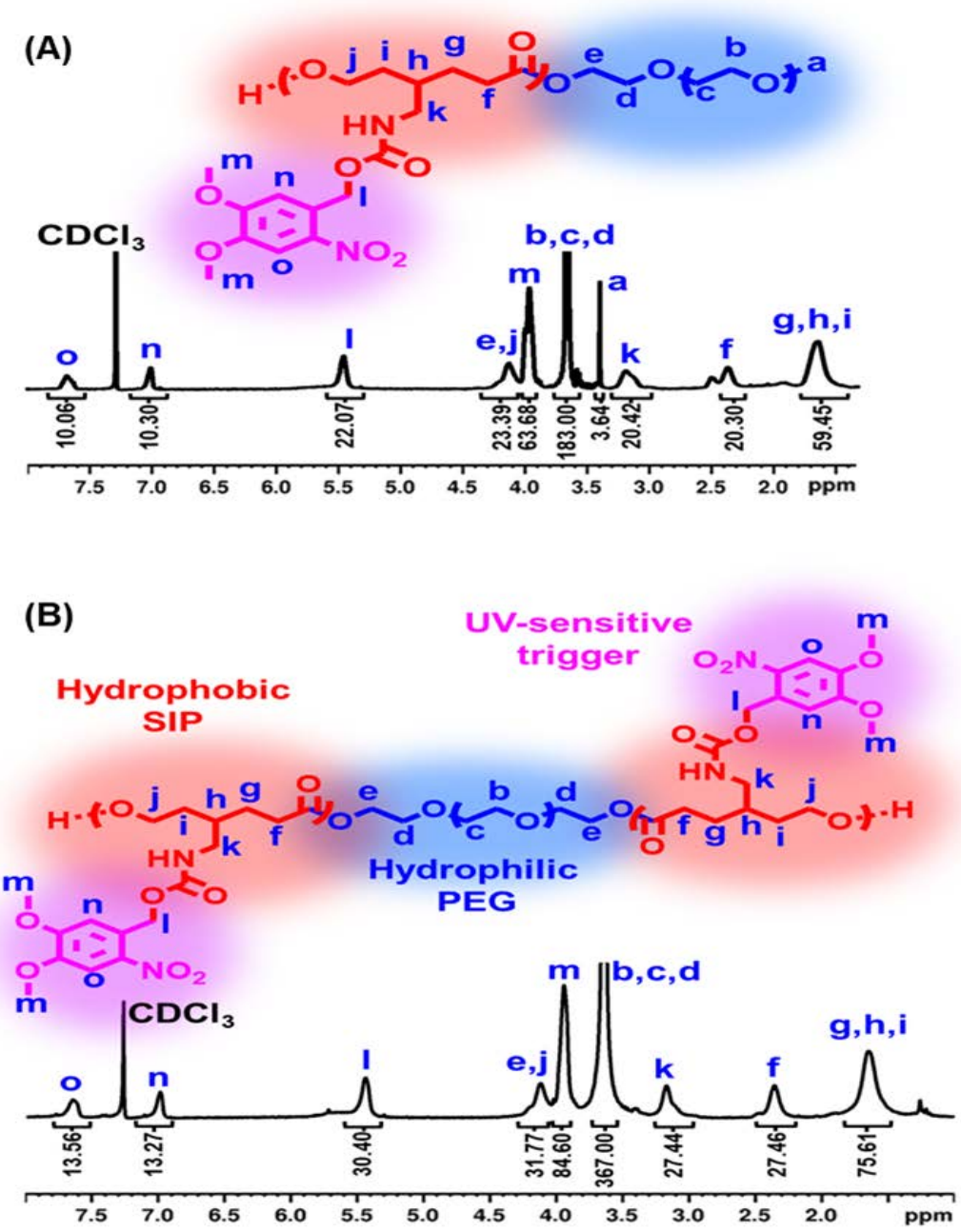

Figure 1. ^{1}H NMR spectra of the amphiphilic diblock (PEG_{2000}-b-SIP_{4000}) and triblock (SIP_{4000}-b-PEG_{4000}-b-SIP_{4000}) UV-sensitive copolymers in $CDCl_3$.

Table 2. Expected molecular weight (M) calculated from the monomer/OH ratio, monomer conversion and DP calculated from ^{1}H NMR spectra of the copolymers, and Đ determined from the SEC traces of the copolymers.

Copolymer or macroinitiator	Monomer/OH ratio	Expected M kg.mol^{-1}	Monomer conv. (%)	DP*	$M_{n,NMR}$* kg.mol^{-1}	Đ
PEG_{2000}-b-SIP_{2000}	6/1	4.2	87	5.7	4.1	1.26
PEG_{2000}-b-SIP_{4000}	12/1	6.5	89	10.2	5.9	1.18
SIP_{2000}-b-PEG_{4000}-b-SIP_{2000}	6/1	8.5	84	10.0	7.2	1.13
SIP_{4000}-b-PEG_{4000}-b-SIP_{4000}	12/1	13.1	89	13.7	9.2	1.11
CH_3-PEG-OH	/	/	/	/	/	1.06
HO-PEG-OH	/	/	/	/	/	1.02

*Calculated from ^{1}H NMR results

Depolymerization of the SIP segments in the copolymers

The depolymerization of the SIP parts in the different copolymer structures was monitored by ^{1}H NMR, UV-vis spectroscopy and SEC. Figure 2 (A) shows the evolution of the ^{1}H NMR spectra of each copolymer as a function of irradiation time. The amplitude of the signals related to the SIP parts decreases gradually with the irradiation time, with notably a complete disappearance of protons located on the nitrobenzyl trigger groups (complete cleavage of the triggers), after an irradiation time of 20-25 minutes. The percentage of cleavage was calculated from the ratio of the signal integrals (noted I) of the trigger protons ($I_{3.17}$,proton k, at 3.17 ppm) and the PEG chain ($I_{3.67}$, protons b, c and d at 3.67 ppm). The calculation was done for diblock and triblock structures according to Equations 1 and 2 respectively. The number of protons of the PEG chains being not the same in the two architectures. $I_{3.17,t0}$ is the value of $I_{3.17}$ before irradiation.

$$\%Cleavage = \left(\frac{I_{3.67}}{183} - \frac{I_{3.17}}{I_{3.17,t0}}\right) \times 100$$ Equation 1

$$\%Cleavage = \left(\frac{I_{3.67}}{367} - \frac{I_{3.17}}{I_{3.17,t0}}\right) \times 100$$ Equation 2

The results reported in Figure 3 (A) show the evolution of this percentage as a function of the irradiation time. For all copolymers, a rapid photocleavage was observed, reaching 100% after 25 minutes. The relationship between cleavage percentage and irradiation time is not linear, this can be explained by the decrease (consumption) in the concentration of the triggering units over the irradiation time. Indeed, at the beginning of the irradiation process a large number of triggering units are available and the cleavage percentage increases quickly, but as the irradiation process progresses the number of available triggering units decreases gradually. Thus, the number of cleavage events decreases gradually, leading to slower and slower increase in the cleavage percentage, until reaching a plateau when all the triggering units are consumed. This graph also shows that, before reaching plateau, the percentage of cleavage of the triggers in the triblocks is higher than in the diblocks, meaning that the architecture of the copolymer has an effect on the rate of cleavage, this can be related to the number of the SIP units that are exposed to UV irradiation. Indeed, for the same number of SIP units, the triblock architectures statistically allow greater exposure of the triggers to UV light, since these units are arranged on both sides of the copolymer chain, unlike diblocks in which the triggers are less spread in space and grouped on the same side of the chain. As consequence and before reaching completion, more cleavage events occurs in triblock architectures than in the case of diblocks.

After having shown the complete cleavage of the triggers, the question was to know if there is a cyclization of the repeating units in the polymer backbones and thus a depolymerization (cleavage of the backbones, mechanism shown in supporting

information Figure S7). In their work on polyurethanes, Kuckling and co-workers[31] demonstrated by ^{1}H NMR the intramolecular cyclization of the backbones after the cleavage of nitrobenzene. Thus, inspired by their work and based on the ^{1}H NMR results obtained here, it can be assumed that the internal cyclization of the SIP backbones was successfully achieved, and that these segments were depolymerized: there is a drastic decrease in the peaks of the SIP segments with appearance of signals corresponding to the six-membered lactam compound (Figure 2(B), circled signals, with PEG_{2000}-b-SIP_{2000} taken as an example).

However, even if the amplitude of the peaks related to the SIP backbones decreases, they do not disappear completely (peaks at 1.67 and 2.40 ppm highlighted in dotted lines in Figure 2 (C) with PEG_{2000}-b-SIP_{4000} taken as an example). This means that a total cleavage of the triggers is reached for all the structures, but the depolymerization of the backbones does not reach completion, some oligomers of the SIP backbone (without triggers) still exist. In order to quantify the residual SIP oligomers, i.e. the depolymerization rates defined as the percentage of cyclized repeating units, the ^{1}H NMR signals related to the SIP backbone ($I_{2.40}$, signals at 2.40 ppm in Figure 2) were integrated and compared to the PEG signals ($I_{3.67}$, at 3.67 ppm in Figure 2) at different irradiation times. The calculation was done for diblock and triblock architectures according to Equations 3 and 4 respectively. $I_{2.40,t0}$ is the value of $I_{2.40}$ before irradiation.

$$\%Depolymerization = \left(\frac{I_{3.67}}{183} - \frac{I_{2.40}}{I_{2.40,t0}}\right) \times 100 \qquad \text{Equation 3}$$

$$\%Depolymerization = \left(\frac{I_{3.67}}{367} - \frac{I_{2.40}}{I_{2.40,t0}}\right) \times 100 \qquad \text{Equation 4}$$

The results are shown in Figure 3 (B). A quick increase in the depolymerization rate is observed at the beginning of the irradiation process (between 0 and 2 minutes), then

the slop of the curves decreases gradually traducing a decrease in the depolymerization kinetics with a tendency to form a plateau without reaching completion. These results are in agreement with those of Almutairi and co-workers[32,33] obtained with two different other chain-chattering self-immolative homopolymers, the authors support the assumption that under irradiation the triggers are first quickly cleaved, then the depolymerization (cyclization) of the backbones occurs more slowly, depending on polarity and pH of the medium, without reaching completion. The two steps (cleavage of the trigger and depolymerization of the backbone) are independent of each other; the first one occurs in response to UV irradiation leading to the formation of pendent amine groups, its conversion rate is complete. Then, to achieve the second step (depolymerization by intramolecular cyclization) the pendent amines make a nucleophilic attack on the ester groups of the backbone (Figure 2). During this second step, the reactivity of amines towards ester groups is affected by the parameters mentioned above, making this step slow and not complete. For these reasons, fragments of SIP oligomers (deprotected) still remain in the irradiated medium.

The maximum depolymerization rates obtained in this work after 25 minutes of irradiation (Figure 3 B) are 42, 44, 47 and 63% for respectively PEG_{2000}-b-SIP_{2000}, PEG_{2000}-b-SIP_{4000}, SIP_{2000}-b-PEG_{4000}-b-SIP_{2000} and SIP_{4000}-b-PEG_{4000}-b-SIP_{4000}. As expected and considering the results of the rates of the trigger's cleavage, long SIP segments offer higher concentration of triggering units in the solution, leading to higher number of triggering events, and thus higher depolymerization rates.

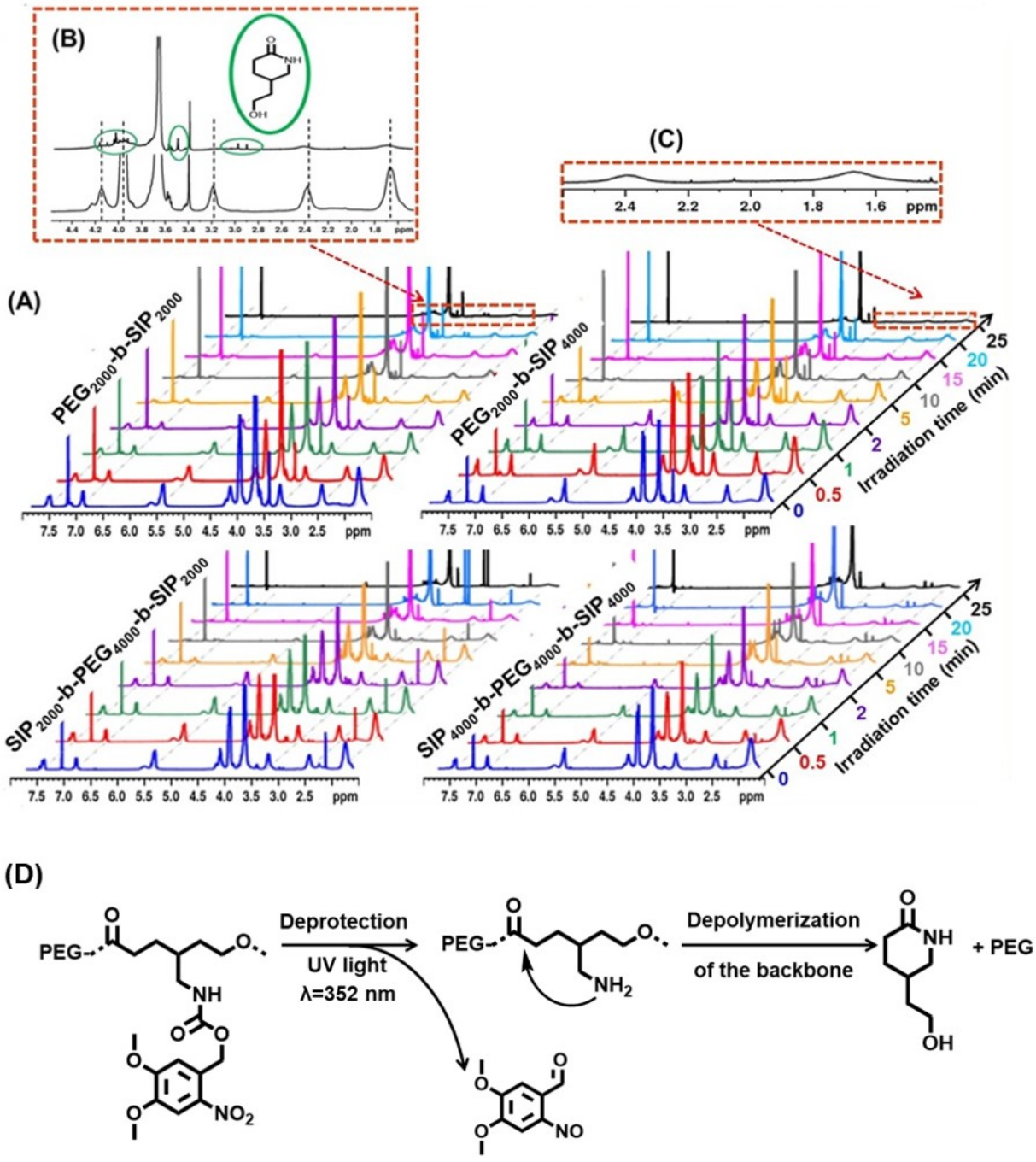

Figure 2. (A):^{1}H NMR spectra of each copolymer as function of irradiation time, in $CDCl_3$. (B): Zoom on the region showing the decrease in the signals related to SIP and the appearance of the peaks related to depolymerization product. (C): The remaining signals of SIP. (D): Schematic representation of the mechanisms of the deprotection and the depolymerization steps.

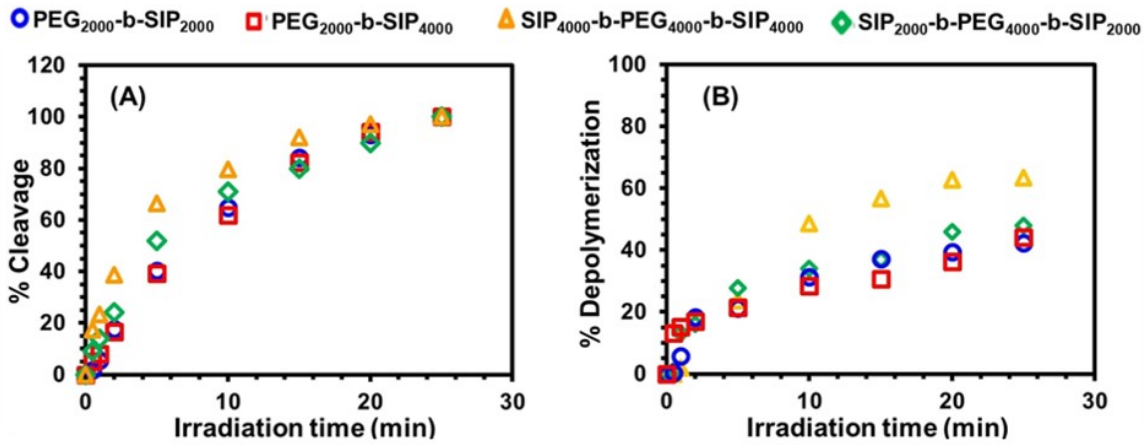

Figure 3. Percentage of the trigger's cleavage (A) and depolymerization of the backbone (B) in the SIP segments as function of irradiation time for each copolymer. Both UV irradiation and the collection of the spectrum were achieved in $CDCl_3$.

The photocleavage of the triggering units was also confirmed by monitoring the intensity of the absorption band of the ONB units at 346 nm by UV-vis spectroscopy (Figure 4). Indeed, a decrease in the absorption intensity with the irradiation time is observed, as well as the concomitant appearance of an absorption band at 400 nm characteristic of the 4,5-dimethoxy-2-nitrobenzaldehyde moieties, which result from the photocleavage of the ONB units,[31,34] as illustrated in Figure 4 (B). No change in the intensity of these two absorption bands was observed after 25 minutes of irradiation, indicating that the cleavage of ONB units reached maximum conversion.

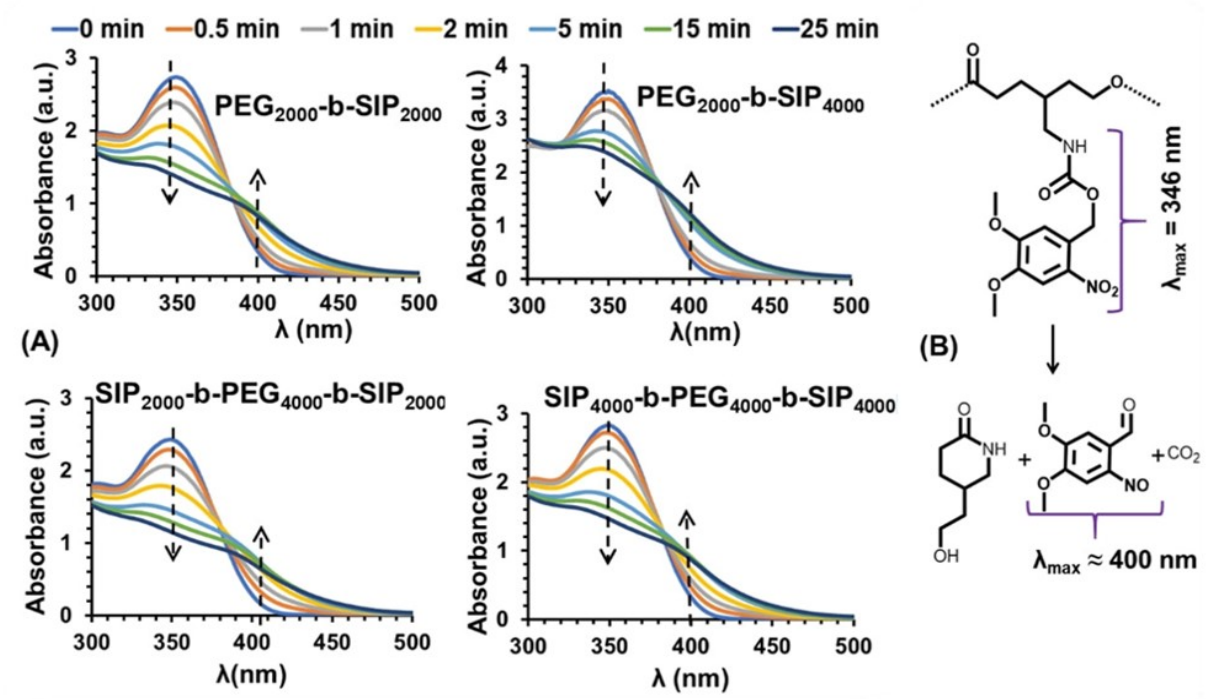

Figure 4. (A): change of the UV-spectra of the different copolymers according to the irradiation time, in chloroform, 0.3 mg.mL^{-1}. (B): molecular structures obtained from the depolymerization of the SIP segments.

Finally, SEC analyzes were carried out to study the impact of irradiation on the depolymerization of copolymers, the results are in Figure 5. The SEC traces recorded after different irradiation times shows a shifting of the signals towards longer retention times, which suggests a decrease in the molecular weights of the copolymers, resulting from both the cleavage of the triggers and the depolymerization of the backbones. The curves stop shifting after 20-25 minutes UV irradiation, in accordance with the ^{1}H NMR and UV-Vis results aforementioned. The same figure shows that the shifting stops before reaching the PEG curves, this means that the depolymerization does not reach completion. It can be assumed that there are chains containing PEG with some SIP units that still remain in the solution, and not only oligomers of SIP separated from the PEG.

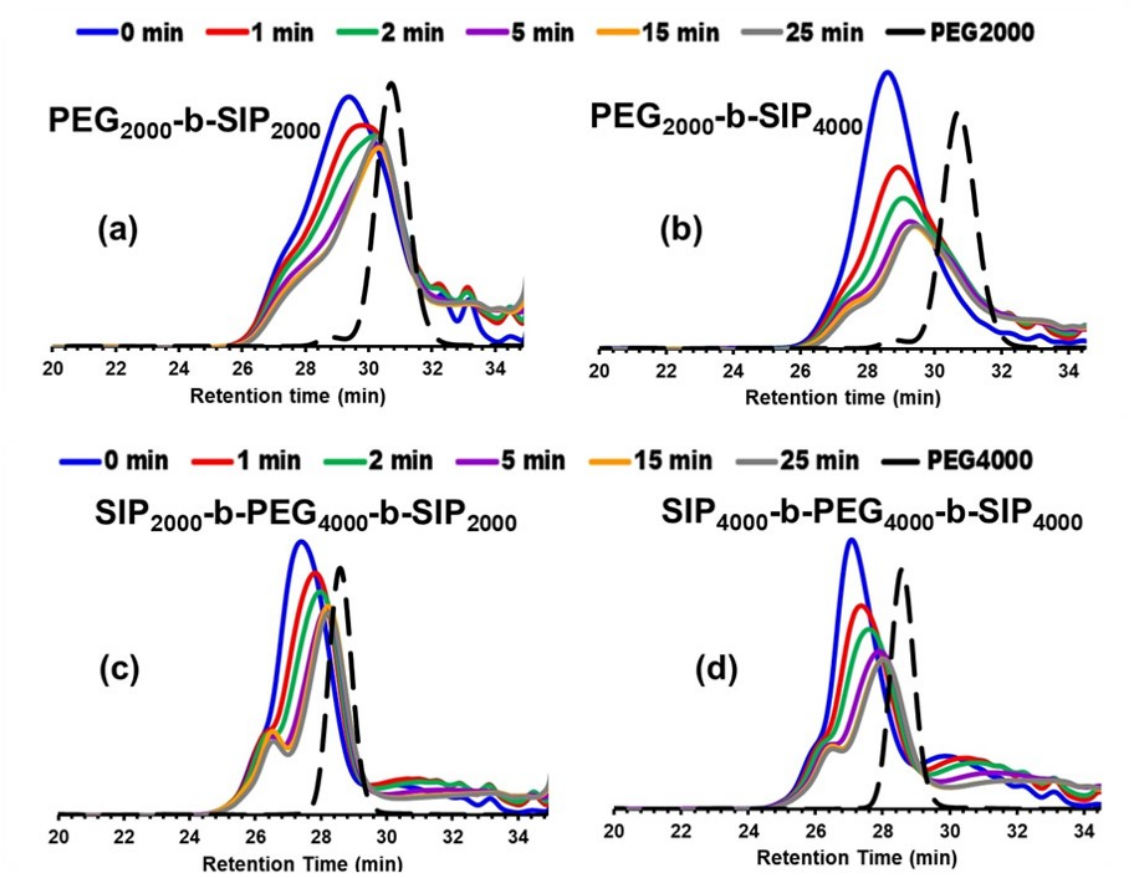

Figure 5. SEC traces at different times of irradiation of PEG_{2000}-b-SIP_{2000} in (A), PEG_{2000}-b-SIP_{4000} in (B), SIP_{2000}-b-PEG_{4000}-b-SIP_{2000} in (C) and SIP_{4000}-b-PEG_{4000}-b-SIP_{4000} in (D). DMF was used as eluent.

Self-assembling behavior

After demonstrating the possibility of UV-depolymerization of block architectures containing SIP segments in organic media, we next sought to show proof of concept that self-assembled constructs could be obtained in both aqueous media and polar organic solvents from SIP-based copolymers, and then disrupted by a photo-induced depolymerization process. This has been exemplified by using the diblock architecture PEG_{2000}-b-SIP_{2000}. Figure 6 shows the DLS curves obtained from analyzing the solutions of the self-assemblies, prepared either by direct dissolution in water (A) or by

direct nanoprecipitation from DCM to ethanol (B), the first measurement was done 24 hours after dissolution/nanoprecipitation as mentioned earlier. In both cases, a single size distribution is detected with however different mean hydrodynamic diameters (D_h)depending on the preparation mode; D_h = 164 nm in the case of direct dissolution in water with narrow distribution and 53 nm in the case of direct nanoprecipitation with a broader distribution. This may be related to the high polarity of water relative to ethanol, which would promote hydrophobic interactions between the SIP blocks, forming larger self-assemblies.[35] Moreover, the diameters of the self-assemblies remain stable for at least 96 hours, testifying to a good stability of the formed nanoobjects. A small deformation is observed in the curves related to the nanoprecipitation process (Figure 6 B), the downward part of the curve shifts slightly towards the small diameters, this shifting can be due to the same reason mentioned above (low polarity of ethanol compared to water, leading to longer stabilization process by the hydrophilic blocks). The critical micellar concentration (CMC) of PEG_{2000}-b-SIP_{2000} was determined by fluorescence measurements; as shown in Figure 6 C, the emission intensity of Nile red was measured in water suspensions containing different concentrations C of the copolymer. The obtained curve (intensity as function of C) shows an inflexion point corresponding to the beginning of the formation of self-assemblies. Two slops were distinguished (before and after the inflection), the intersection of the two slops gave us the value of CMC which is 0.12 $mg.mL^{-1}$. For all the experiments involving self-assembling of PEG_{2000}-b-SIP_{2000} in this work, the concentration of the copolymer was of 1 $mg.mL^{-1}$, i.e. about 8 times higher than the CMC.

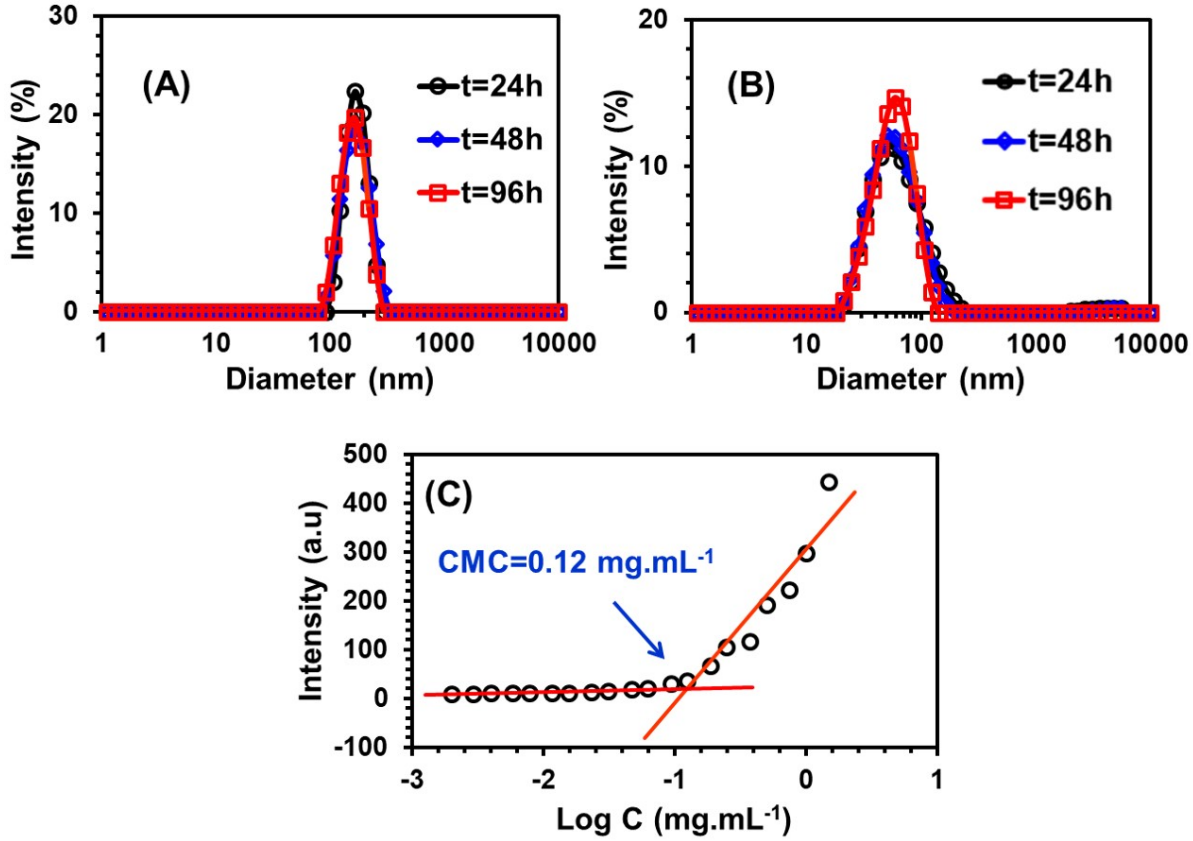

Figure 6. Intensity distribution, from DLS, of the solutions of the self-assemblies obtained by direct dissolution in water (A) and by direct nanoprecipitation (B) of the PEG_{2000}-b-SIP_{2000} copolymer. (C): Intensity of the fluorescence emission spectra of Nile red as a function of the logarithm of the concentration C of PEG_{2000}-b-SIP_{2000}. The excitation wavelength was λ_{ex} = 555 nm, the emission wavelength was λ_{em} = 635 nm.

UV-triggered disassembly of the self-assemblies

The study of UV-triggered disassembly of SIP-based nanoobjects was performed by monitoring the derived count rate (DCR), measured by DLS, in aqueous media. This DCR is a parameter reporting the intensity of the scattered light which depends on the number and size of scattering species in solution.[25] The results reported in Figure 7 show the evolution of the DCR of the solutions, containing the irradiated or non-irradiated self-assemblies, as a function of irradiation time. Except for slight fluctuations, the DCR of non-irradiated solutions remained stable over time for both

self-assemblies. In contrast, a rapid drop in the DCR value was observed under UV irradiation, reaching a plateau after 4 minutes for self-assemblies prepared by direct dissolution in water (A), and after 2.25 minutes for self-assemblies prepared by direct nanoprecipitation (B). This trend indicated the formation of smaller polymer structures compared to starting nano-objects, likely due to the depolymerization of the hydrophobic SIP block and therefore the disassembly of self-assemblies under UV irradiation. Faster disruption was observed in ethanol, probably because the self-assemblies were less stabilized in ethanol compared to water due its lower polarity, so that a small disturbance (depolymerization/cleavage of the trigger) in the hydrophobic core is enough to trigger a disassembly. Visually, insoluble macroscopic aggregates can be observed in the solution after irradiation, suggesting the release of hydrophobic fragments.

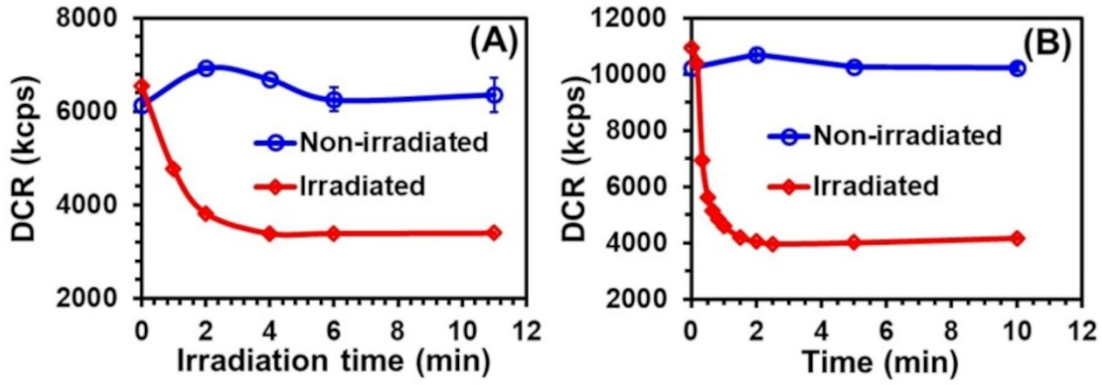

Figure 7. Derived count rate (DCR) monitoring by DLS, for irradiated and non-irradiated suspensions of self-assemblies, prepared bay direct dissolution in water (A) or by direct nanoprecipitation from DCM to ethanol (B).

To further support these results, Tyndall effect tests were achieved. This effect corresponds to the scattering of light by particles in solution (or in light-transmitting media) when the incident beam wavelength is of the same order as the particles' seize. For these tests, we chose a red laser beam (650 nm, 1 mW) which does not interfere with the triggerable SIP units. Figure 8, shows that the red laser beam appears as a straight line crossing the non-irradiated solution, and it disappears when the same solution is irradiated (the irradiation time was set according to the DCR results discussed above: 2 minutes and 15 seconds for the self-assemblies obtained by direct nanoprecipitation and 5 minutes for those obtained by direct dissolution in water). This observation further supports the previous results and confirm the disintegration of the self-assemblies under UV-light.

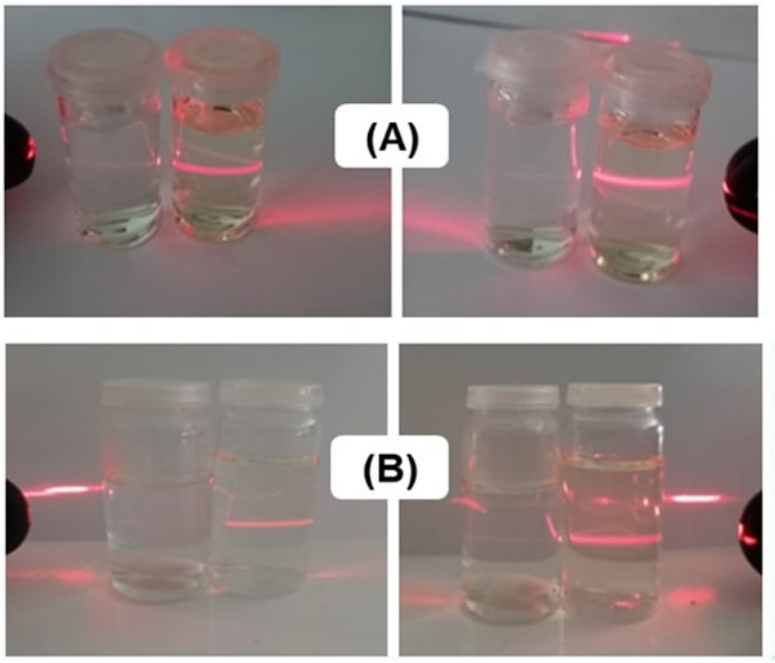

Figure 8. Pictures showing the scattered laser beam by the self-assemblies (Tyndall effect). The solutions were prepared either by direct dissolution of the copolymer in water (A) or by direct nanoprecipitation (B). For each case (A and B), the glasses containing irradiated or non-irradiated solutions were put next to each other and the

laser beam was applied from one side then the other of the whole. The laser beam appears in the non-irradiated solution but not in the irradiated one, regardless of the direction of the laser.

SEM images of the dried self-assemblies are shown in Figure 9. Nanoparticles with mean diameters (D_{SEM}) of 77 ± 31 nm and 39 ± 15 nm are obtained from solutions in water and ethanol respectively. These values were calculated from populations of 100 nanoparticles. The size distributions are also shown in the same figure. There is a noticeable difference between the diameters obtained by the two techniques, D_{DLS} is higher than D_{SEM} by a factor of 2.1 and 1.4 for respectively the first and second preparation method. This decrease in the nanoparticle size upon drying has been noted in literature[36] and attributed to the swelling character of the nanoparticles in the solvents. However, the observation that larger assemblies were obtained in water compared to ethanol still coherent between the two techniques. Furthermore, the size distributions calculated from SEM are not in accordance with the DLS curves, in the way that direct dissolution method gives narrow distribution in DLS compared to broader distributions for the direct nanoprecipitation, inversely to the SEM results. These phenomena have already been mentioned in literature[37], DLS provides hydrodynamic diameters from a measurement over a volume, it is a meaningful method to characterize similar and monodisperse particles and becomes inadequate for populations with multimodal or large distributions. In this sense, imaging method like SEM is more suitable to reveal the presence of several populations of large distributions and presents a complementary analysis, but drying can promote size redistribution due to capillary forces, size-dependent adsorption on the metallic surface of the stub during the evaporation of the solvent, and deformation of the particles. All these factors, combined to the effects of image magnification and the viewing angle,

lead to limited populations of objects that are statistically non-relevant and different from those obtained by DLS.

Figure 9 shows also the comparison between irradiated and non-irradiated samples. The comparison highlights a drastic decrease in the number of nanoparticles due to the UV irradiation, confirming the UV-triggered disintegration of the self-assemblies.

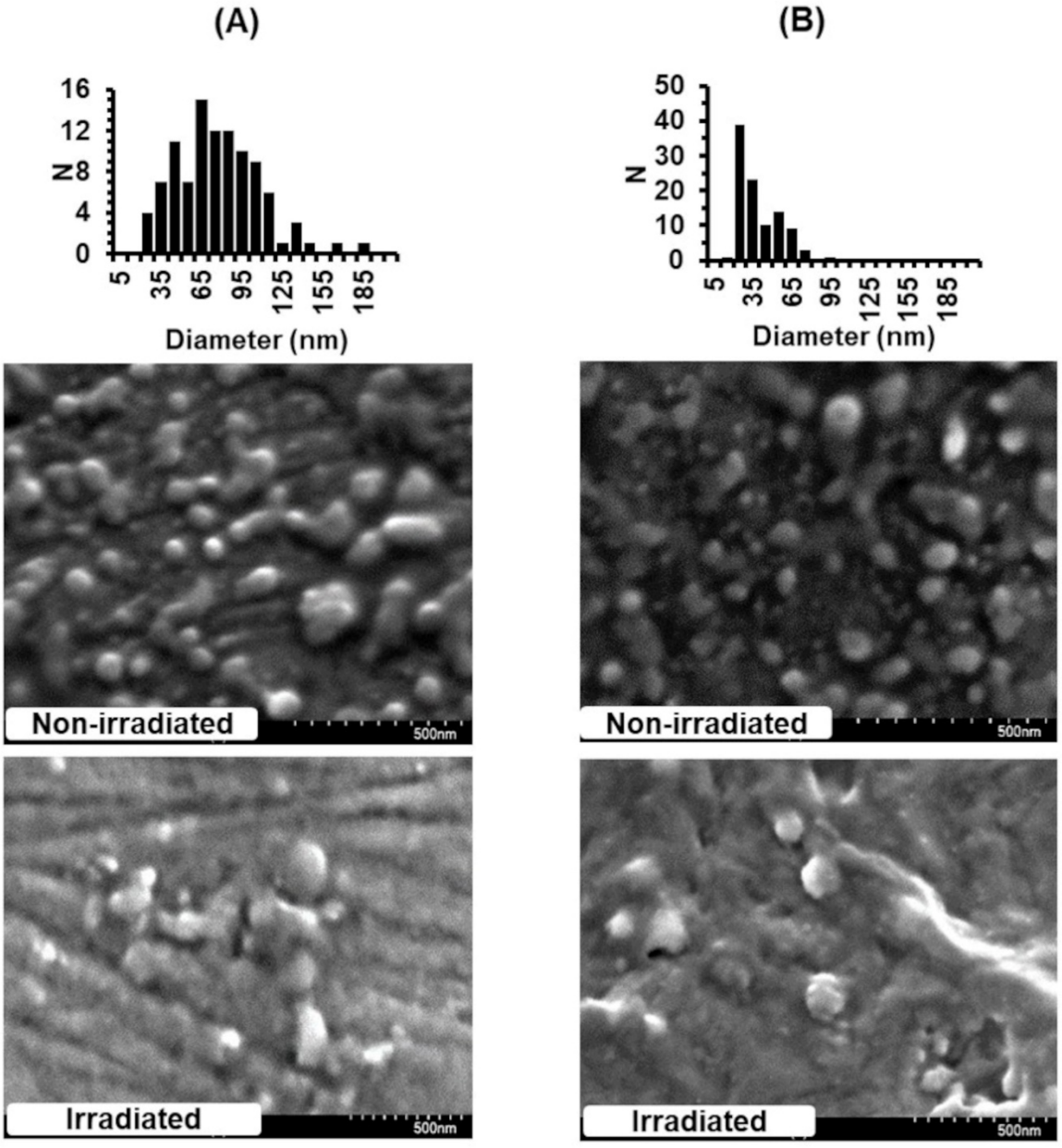

Figure 9. Size distributions of the nanoparticles and SEM images before and after UV-irradiation. The solutions of self-assemblies were prepared either by direct dissolution in water (A) or by direct nanoprecipitation from DCM to ethanol (B).

The products of the disintegration of the self-assemblies were analyzed by ^{1}H NMR, a comparative analysis was carried on three samples self-assemblies of PEG_{2000}-b-SIP_{2000} in water, the first was kept as control sample (non-irradiated), the second one was irradiated for 5 minutes and the third was irradiated for 25 minutes. The water was evaporated from the three samples and the obtained residues were dried under vacuum until removing all the water traces. The ^{1}H NMR spectra of the three residues are in Supporting Information Figure S8, showing that the irradiation of the self-assemblies causes both cleavage of the triggers (%Cleavage ≈64%) and the depolymerization of the SIP backbones (%Depolymerization = 31%) after 5 minutes of irradiation, these two percentages increase respectively until ~100% and 43 % after 25 irradiation. Meaning that the two phenomena (cleavage and depolymerization) occur in parallel causing the disruption of the self-assemblies.

Encapsulation and UV-triggered release of Nile red from the self-assemblies

To examine the potential for the system to encapsulate and release hydrophobic payload upon irradiation, Nile red was used as hydrophobic model molecule and incorporated to the self-assemblies. Figure 10 shows visually the comparison between two suspensions in water, one containing only Nile red (A) and the other contains Nile red with PEG_{2000}-b-SIP_{2000} based self-assemblies. The difference in color indicates that the Nile red was encapsulated in the hydrophobic cores of the self-assemblies. The suspension of slef-assemblies containing Nile red was subjected to UV-irradiation with monitoring the evolution of the emission spectrum of the Nile red, Figure 10 C shows

the results. The emission intensity of the Nile red decreases gradually with the irradiation time, this decrease reaches 86% of the initial value after 25 minutes irradiation, no considerable changes were observed after this time. Moreover, the emission spectrum of the non-irradiated suspension was collected 24 hours after the incorporation of the Nile red (Non irr. in Figure 10 C), and it remained almost identical to the spectrum at t=0. This result shows that there was a release of Nile red from the self-assemblies due to the UV irradiation, and that the amount of the released Nile red could be controlled by setting the irradiation time.

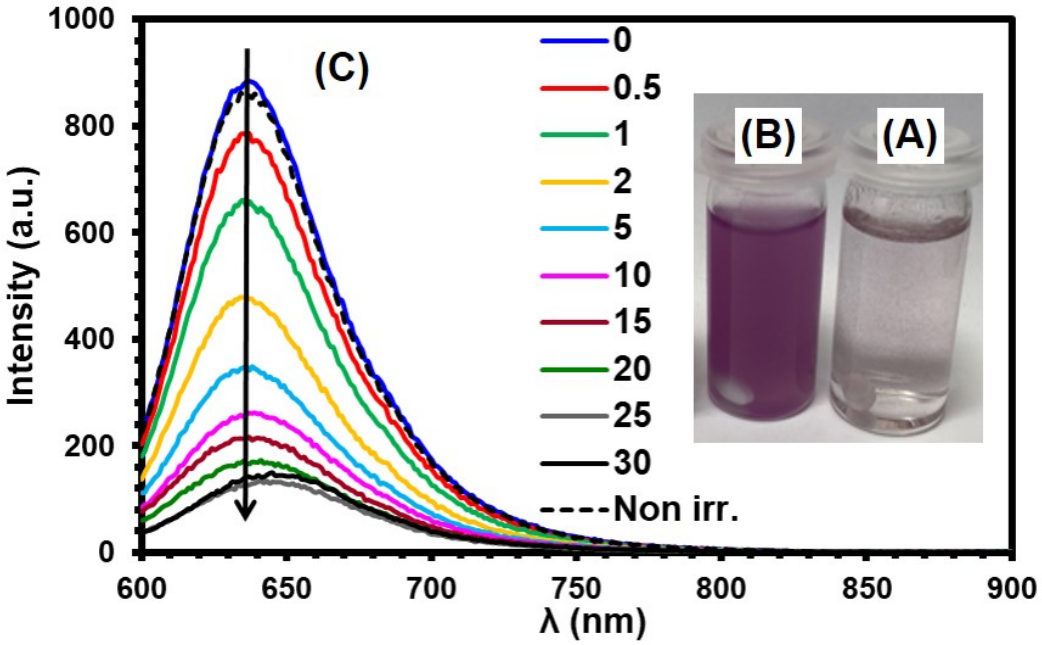

Figure 10. Photography of (A): a suspension of Nile red in water, (B): a suspension of Nile red in water containing 1mg.mL^{-1} of PEG_{2000}-b-SIP_{2000}. (C): Emission spectra of the suspension of self-assemblies containing Nile red at different irradiation times (the numbers indicate the irradiation time in minutes). The excitation wavelength was 555 nm. The doted line (Non irr.) corresponds to a non-irradiated sample analyzed 24 four hours after it's preparation.

The side product released during the deprotection of the SIP is 4,5-dimethoxy-2-nitroso-benzaldehyde as shown in Figure 2 D. This molecule results from the cleavage of the trigger. The protective group used in this work (DMNBA) and its derivatives are among the most commonly used in biological research. [32,38-40] Some studies have shown that this protective group have almost no cytotoxicity after cleavage. [41,42] Other studies demonstrated that its cytotoxicity appears only at high concentrations; Pinchuck et al. [43] used DMNBA as UV-sensitive cleavable group in caged prodrugs of vascular endothelial growth factor receptor (VEGFR-2). The release of VEGFR-2 was accompanied by the release of 4,5-dimethoxy-2-nitroso-benzaldehyde (the same side product as in this work), the authors demonstrated that this residue becomes cytotoxic only when the concentration of the caged prodrug exceeds its efficacious concentration by a factor of 500. Horbert et al. [44] developed photoactivatable prodrugs of antimelanoma agent vermurafenib by using DMNBA as UV-sensitive cleavable group, the authors showed that the released nitroso compound (the same as in this work) becomes cytotoxic when the concentration of the caged prodrugs is 100-fold higher than the efficacious concentration for the treatment.

CONCLUSION

Amphiphilic diblock and triblock copolymers, containing hydrophilic PEG and hydrophobic SIP segments of different chain-lengths, were synthesized by ROP. The SIP blocks are UV-sensitive and able to undergo triggered cleavage of the methoxynitrobenzyl group and depolymerization of the backbone by intramolecular cyclization, following a chain chattering self-immolative reaction.

Complete cleavage of the triggers was reached after 20-25 minutes depending on the structure of the copolymers, the depolymerization rates of the backbones reached values between 42 and 63%. To favor the depolymerization reaction of the SIP backbones and increase the depolymerization rates, it may be suitable to achieve these reactions in media with pH lightly higher than 7, this basicity can favor the nucleophilic attack of the deprotected amine on the ester function of the backbone and then increase the cyclization kinetics[33]. Increasing the polarity if the environment, by changing solvents or making mixture of solvents, can also favor the depolymerization of the backbone through cyclization reactions,[34] with respect to the solubility of the copolymers.

By designing amphiphilic block architectures, it was possible to make stable self-assemblies from the diblock copolymers by different methods, the possibility to disintegrate them in a triggered and rapid manner was demonstrated by different techniques. A quick disintegration of the self-assemblies was observed, up to 135 seconds under UV-light at 352 nm wavelength.

In comparison with the systems developed in literature, the self-assemblies developed in this work allow faster disassembling kinetics under stimulus, and higher control. This was possible by using a different mechanism of the depolymerization of the SIP chains

in the amphiphilic copolymers: chain-chattering depolymerization mechanism, ensured by incorporating a trigger in each repeating unit of the SIP backbone, rather than a head-to-tail depolymerization mechanism, caused by a unique trigger at the chain end of the SIP.

From the fundamental point of view, these results can contribute to the extension of the studies on SIPs, so far focused on chemistry and development of monomers, to the design of macromolecular architectures in order to modulate and control their physicochemical and physical properties, with the aim to make them processable and useful in different applications.

Regarding the applicative aspects, this study is a proof of concept showing the possibility to make UV-triggerable self-assemblies allowing quick disintegration, this behavior can be exploited to initiate works on drug-loaded nanoparticles for triggered and controlled drug-release. The architecture developed here will be tested for this purpose in a coming study.

ACKNOWLEDGMENT

The Chevreul Institute is thanked for its help in the development of this work through the ARCHI-CM project supported by the “Ministère de l’Enseignement Supérieur, de la Recherche et de l’Innovation”, the region “Hauts-de-France”, the ERDF program of the European Union and the “Métropole Européenne de Lille”.

This work was also partly funded by the UMET laboratory (Unité Matériaux Et Transformations, UMR 8207) and by Centrle Lille Institut.

The authors thank Dr. Ahmed Addad and Dr. Alexandre Fadel for their help in carrying out the work on the electron microscopy facility of the Advanced Characterization

Platform of the Chevreul Institute. The authors thank Aurélie Malfait and Maxence Epinat for the SEC analyzes.

SUPPORTING INFORMATION

Reaction scheme of the synthesis of the monomer, synthesis procedure of compound 1, ^{1}H NMR spectrum of compounds 1, synthesis procedure of compound 3, ^{1}H NMR spectrum of compound 3, synthesis procedure of compound 4, ^{1}H NMR spectrum of compound 4, ^{13}C NMR spectrum of compound 4, calculation method of the monomer conversion, SEC traces of the copolymers, reaction scheme of ONB cleavage and backbone depolymerization, ^{1}H NMR spectra of the residues obtained after the irradiation of self-assemblies of PEG_{2000}-b-SIP_{2000}.

REFERENCES

(1) Phan, H.; Cavanagh, R.; Destouches, D.; Vacherot, F.; Brissault, B.; Taresco, V.; Penelle, J.; Couturaud, B. H2O2-Responsive Nanocarriers Prepared by RAFT-Mediated Polymerization-Induced Self-Assembly of N-(2-(Methylthio)ethyl)acrylamide for Biomedical Applications. *ACS Appl. Polym. Mater*. **2022**, 4 (10), 7778-7789. DOI: 10.1021/acsapm.2c01327.

(2) Lee, S.; Lee, Y.; Kim, E-.M.; Nam, K. W.; Choi, I. Aqueous-Phase Synthesis of Hyaluronic Acid-Based Hydrogel Nanoparticles for Molecular Storage and Enzymatic Release. *ACS Appl. Polym. Mater*. **2020**, 2 (2), 342-350. DOI: 10.1021/acsapm.9b00834.

(3) Saha, B.; Bhattacharyya, S.; Mete, S.; Mukherjee, A.; De, Priyadarsi. Redox-Driven Disassembly of Polymer–Chlorambucil Polyprodrug: Delivery of Anticancer Nitrogen Mustard and DNA Alkylation. *ACS Appl. Polym. Mater*. **2019**, 1 (9), 2503-2515.

(4) Esser-Kahn, A. P.; Odom, S. A.; Sottos, N. R.; White, S. R.; Moore, J. S. Triggered Release from Polymer Capsules. *Macromolecules* **2011**, *44* (14), 5539–5553. DOI: 10.1021/ma201014n.

(5) El-Sawy, H. S.; Al-Abd, A. M.; Ahmed, T. A.; El-Say, K. M.; Torchilin, V. P. Stimuli-Responsive Nano-Architecture Drug-Delivery Systems to Solid Tumor Micromilieu: Past, Present, and Future Perspectives. *ACS Nano* **2018**, *12* (11), 10636–10664. DOI: 10.1021/acsnano.8b06104.

(6) Patra, J. K.; Das, G.; Fraceto, L. F.; Campos, E. V. R.; Rodriguez-Torres, M. del P.; Acosta-Torres, L. S.; Diaz-Torres, L. A.; Grillo, R.; Swamy, M. K.; Sharma, S.; Habtemariam, S.; Shin, H.-S. Nano Based Drug Delivery Systems: Recent Developments and Future Prospects. *Journal of Nanobiotechnology* **2018**, *16* (1), 71. DOI: 10.1186/s12951-018-0392-8.

(7) Chen, Y.; Zhang, Z.-H.; Han, X.; Yin, J.; Wu, Z.-Q. Oxidation and Acid Milieu-Disintegratable Nanovectors with Rapid Cell-Penetrating Helical Polymer Chains for Programmed Drug Release and Synergistic Chemo-Photothermal Therapy. *Macromolecules* **2016**, *49* (20), 7718–7727. DOI: 10.1021/acs.macromol.6b02063.

(8) Shen, X.; Cao, S.; Zhang, Q.; Zhang, J.; Wang, J.; Ye, Z. Amphiphilic TEMPO-Functionalized Block Copolymers: Synthesis, Self-Assembly and Redox-Responsive Disassembly Behavior, and Potential Application in Triggered Drug Delivery. *ACS Appl. Polym. Mater*. **2019**, 1 (9), 2282-2290. DOI: 10.1021/acsapm.9b00293.

(9) Karlsson, J.; Vaughan, H. J.; Green, J. J. Biodegradable Polymeric Nanoparticles for Therapeutic Cancer Treatments. *Annu Rev Chem Biomol Eng* **2018**, *9*, 105–127. DOI: 10.1146/annurev-chembioeng-060817-084055.

(10) Santra, S.; Shaw, Z.; Narayanam, R.; Jain, V.; Banerjee, T. Selective O-Alkylation of 2,2′-Bis(hydroxymethyl)propionic Acid to Synthesize Biodegradable

Polymers for Drug Delivery Applications. *ACS Appl. Polym. Mater*. **2020**, 2 (8), 3465-3473. DOI: 10.1021/acsapm.0c00509.

(11) Su, S.; Kang, P. M. Systemic Review of Biodegradable Nanomaterials in Nanomedicine. *Nanomaterials (Basel)* **2020**, *10* (4), 656. DOI: 10.3390/nano10040656.

(12) Jeevitha, D.; Amarnath, K. Chitosan/PLA Nanoparticles as a Novel Carrier for the Delivery of Anthraquinone: Synthesis, Characterization and in Vitro Cytotoxicity Evaluation. *Colloids and Surfaces B: Biointerfaces* **2013**, *101*, 126–134. DOI: 10.1016/j.colsurfb.2012.06.019.

(13) Wu, C.; Fu, J.; Zhao, Y. Novel Nanoparticles Formed via Self-Assembly of Poly(Ethylene Glycol-b-Sebacic Anhydride) and Their Degradation in Water. *Macromolecules* **2000**, *33* (24), 9040–9043. DOI: 10.1021/ma000989+.

(14) Zhu, Y.; Yang, B.; Chen, S.; Du, J. Polymer vesicles : Machanism, preparation, application , and responsive behavior. *Prog. Polym. Sci*. **2017**, 64 , 1-22. DOI: 10.1016/j.progpolymsci.2015.05.001.

(15) Yin, J.; Chen, Y.; Zhang, Z-. H.; Han, X. Stimuli-Responsive Block Copolymer-Based Assemblies for Cargo Delivery and Theranostic Applications. *Polymers* **2016**, 8 (7), 268. DOI: 10.3390/polym8070268.

(16) Jiang, C.; Xu, G.; Gao, J. Stimuli-Responsive Macromolecular Self-Assembly. *Sustainability* **2022**, 14 (18), 11738. DOI: 10.3390/su141811738.

(17) Marturano, V.; Cerruti, P.; Giamberini, M.; Tylkowski, B.; Ambrogi, V. Light-Responsive Polymer Micro- and Nano-Capsules. *Polymers (Basel)* **2016**, *9* (1), 8. DOI: 10.3390/polym9010008.

(18) Bertrand, O.; Gohy, J.-F. Photo-Responsive Polymers: Synthesis and Applications. *Polym. Chem.* **2016**, *8* (1), 52–73. DOI: 10.1039/C6PY01082B.

(19) Zhou, S.; Ding, C.; Wang, C.; Fu, J. UV-Light Cross-Linked and PH de-Cross-Linked Coumarin-Decorated Cationic Copolymer Grafted Mesoporous Silica Nanoparticles for Drug and Gene Co-Delivery in Vitro. *Materials Science and Engineering: C* **2020**, *108*, 110469. DOI: 10.1016/j.msec.2019.110469.

(20) Lu, D.; Zhu, M.; Wu, S.; Wang, W.; Lian, Q.; R. Saunders, B. Triply Responsive Coumarin-Based Microgels with Remarkably Large Photo-Switchable Swelling. *Polymer Chemistry* **2019**, *10* (20), 2516–2526. DOI: 10.1039/C9PY00233B.

(21) Zhu, J.; Guo, T.; Wang, Z.; Zhao, Y. Triggered Azobenzene-Based Prodrugs and Drug Delivery Systems. *Journal of Controlled Release* **2022**, *345*, 475–493. DOI: 10.1016/j.jconrel.2022.03.041.

(22) Santra, S.; Ghosh, A.; Mondal, A.; Ali, S. M.; Das, D.; Sarkar, K. ; Roy, L. ; Molla, M. R. Stabilizing Entropically Driven Self-Assembly of Self-Immolative Polyurethanes in Water: A Strategy for Tunable Encapsulation Stability and Controlled Cargo Release. *ACS Appl. Polym. Mater*. **2022**, 4 (10), 7614-7625. DOI: 10.1021/acsapm.2c01261.

(23) Yardley, R. E.; Kenaree, A. R.; Gillies, E. R. Triggering Depolymerization: Progress and Opportunities for Self-Immolative Polymers. *Macromolecules* **2019**, *52* (17), 6342–6360. DOI: 10.1021/acs.macromol.9b00965.

(24) Sagi, A.; Weinstain, R.; Karton, N.; Shabat, D. Self-Immolative Polymers. *J. Am. Chem. Soc.* **2008**, *130* (16), 5434–5435. DOI: 10.1021/ja801065d.

(25) Liang, X.; Gillies, E. R. Self-Immolative Amphiphilic Diblock Copolymers with Individually Triggerable Blocks. *ACS Polym. Au* **2022**. DOI: 10.1021/acspolymersau.2c00013.

(26) Ding, Z.; Cen, J.; Wu, Y.; Zhong, K.; Liu, G.; Hu, J.; Liu, S. Self-Immolative Nanoparticles for Stimuli-Triggered Activation, Covalent Trapping and Accumulation of in Situ Generated Small Molecule Theranostic Fragments. *Giant* **2020**, *1*, 100012. DOI: 10.1016/j.giant.2020.100012.

(27) Mutlu, H.; Barner-Kowollik, C. Green Chain-Shattering Polymers Based on a Self-Immolative Azobenzene Motif. *Polym. Chem.* **2016**, *7* (12), 2272–2279. DOI: 10.1039/C5PY01937K.

(28) Xiao, Y.; Tan, X.; Li, Z.; Zhang, K. Self-Immolative Polymers in Biomedicine. *J. Mater. Chem. B* **2020**, *8* (31), 6697–6709. DOI: 10.1039/D0TB01119C.

(29) Tong, R.; Chiang, H. H.; Kohane, D. S. Photoswitchable Nanoparticles for in Vivo Cancer Chemotherapy. *Proceedings of the National Academy of Sciences* **2013**, *110* (47), 19048–19053. DOI: 10.1073/pnas.1315336110.

(30) Du, J.; Lu, H. Polymeric Micells. in *Encyclopedia of Polymer Science and Technology*. ed. M. Peterca. Wiley, **2012**. DOI: 10.1002/0471440264.pst547.

(31) Sun, J.; Rust, T.; Kuckling, D. Light-Responsive Serinol-Based Polyurethane Nanocarrier for Controlled Drug Release. *Macromolecular Rapid Communications* **2019**, *40*. DOI: 10.1002/marc.201900348.

(32) Fomina, N.; McFearin, C.; Sermsakdi, M.; Edigin, O.; Almutairi, A. UV and Near-IR Triggered Release from Polymeric Nanoparticles. *J. Am. Chem. Soc.* **2010**, *132* (28), 9540–9542. DOI: 10.1021/ja102595j.

(33) Fomina, N.; McFearin, C. L.; Sermsakdi, M.; Morachis, J. M.; Almutairi, A. Low Power, Biologically Benign NIR Light Triggers Polymer Disassembly. *Macromolecules* **2011**, 44 (21), 8590-8597. DOI: 10.1021/ma201850q.

(34) de Gracia Lux, C.; McFearin, C. L.; Joshi-Barr, S.; Sankaranarayanan, J.; Fomina, N.; Almutairi, A. Single UV or Near IR Triggering Event Leads to Polymer Degradation into Small Molecules. *ACS Macro Lett.* **2012**, *1* (7), 922–926. DOI: 10.1021/mz3002403.

(35) Gacem, N.; Diao, P. Effect of Solvent Polarity on the Assembly Behavior of PVP Coated Rhodium Nanoparticles. *Colloids and Surfaces A: Physicochemical and Engineering Aspects* **2013**, *417*, 32–38. DOI: 10.1016/j.colsurfa.2012.10.055.

(36) Korchia, L.; Lapinte, V.; Travelet, C.; Borsali, R.; Robin, J.-J.; Bouilhac, C. UV-Responsive Amphiphilic Graft Copolymers Based on Coumarin and Polyoxazoline. *Soft Matter* **2017**, *13* (25), 4507–4519. DOI: 10.1039/C7SM00682A.

(37) Belkhir, K.; Cerlati, O.; Heaugwane, D.; Tosi, A.; Benkhaled, B. T.; Brient, P.-L.; Chatard, C.; Graillot, A.; Catrouillet, S.; Balor, S.; Goudounèche, D.; Payré, B.; Laborie, P.; Lim, J.-H.; Putaux, J.-L.; Vicendo, P.; Gibot, L.; Lonetti, B.; Mingotaud, A.-F.; Lapinte, V. Synthesis and Self-Assembly of UV-Cross-Linkable Amphiphilic Polyoxazoline Block Copolymers: Importance of Multitechnique Characterization. *Langmuir* **2022**, *38* (51), 16144–16155. DOI : 10.1021/acs.langmuir.2c02896.

(38) Huu, V. A. N.; Luo, J.; Zhu, J.; Zhu, J.; Patel, S.; Boone, A.; Mahmoud, E.; McFearin, C.; Olejniczak, J.; de Gracia Lux, C.; Lux, J.; Fomina N.; Huynh, M.; Zhang, K.; Almutairi, A.; Light-responsive nanoparticle depot to control release of a small molecule angiogenesis inhibitor in the posterior segment of the eye. *J. Control. Release* **2015**, 200, 71-77. Doi: 10.1016/j.jconrel.2015.01.001.

(39) Li, J.; Xiao, D.; Xie, F. ; Li, W. ; Zhao, L. ; Sun, W. ; Yang, X.; Zhou, X. Novel antibody-drug conjugate with UV-controlled cleavage mechanism for cytotoxin release. *Bioorg. Chem.* **2021**, 111, 104475. DOI: 10.1016/j.bioorg.2020.104475.

(40) Kaplan, J. H.; Forbuch, B.; Hoffman, J. F. Rapid photolytic release of adenosine 5’-triphosphate from a protected analog: utilization by the sodium:potassium pump of human red blood cell ghosts. *Biochemistry* **1978**, 17 (10), 1929-1935. DOI: 10.1021/bi00603a020.

(41) Shin, W.; Han, J.; Kumar, R.; Lee, G. G.; Sessler, J. L.; Kim, J-. H.; Kim, J. S. Programmed activation of cancer cell apoptosis: A tumor-targeted phototherapeutic topoisomerase I inhibitor. *Sci. Rep.* **2016**, 6, 29018. DOI: 10.1038/srep29018.

(42) Ibsen, S.; Zahavy, E.; Wrasdilo, W.; Berns, M.; Chan, M.; Esener, S.; A novel Doxorubicin prodrug with controllable photolysis activation for cancer chemotherapy. *Pharm. Res.* **2010**, 27 (9), 1848-1860. DOI: 10.1007/s11095-010-0183-x.

(43) Pinchuk, B.; Horbert, R.; Döbber, A.; Kuhl, L.; Peifer, C. Photoactivatable Caged Prodrugs of VEGFR-2 Kinase Inhibitors. *Molecules* **2016**, 21 (5), 570. DOI: 10.3390/molecules21050570.

(44) Horbert, R.; Pinchuk, B.; Davies, P.; Alessi, D. R.; Peifer, C. Photoactivatable prodrugs of antimelanoma agent vemurafenib. *ACS Chem. Bio.* **2015**, 10 (9), 2099-2107. DOI: 10.1021/acschembio.5b00174.